Adaptive Control Method to Manage SOC for Energy Storage in DC Electric Railways

Hammad Alnuman, Daniel T. Gladwin, Martin P. Foster, and Thomas Fantham
Department of Electronic and Electrical Engineering
University of Sheffield
Sheffield, United Kingdom
hhalnuman1@sheffield.ac.uk

***Abstract*—Incorporating energy storage systems (ESSs) into electric railways has been shown to be advantageous for energy saving and power quality enhancement. For DC railways, the connection method of the ESS to the track may impose restrictions on charging and discharging the ESS to control the state of charge (SOC). Without management of the SOC, the ESS is shown in this study to reach minimum or maximum limits, reducing its effectiveness due to unavailability. Whilst it is possible to oversize the capacity of ESS, this incurs increased costs and requires more physical space. The main objective of this study is to propose and validate a control algorithm that prevents the ESS from reaching the maximum or minimum SOC limits whilst maintaining the benefits of the system. The main concept of the proposed control method is to dynamically update the voltage and current setpoints of the ESS to manage its SOC. The control algorithm is implemented in the MATLAB software and the simulation results are validated against experimental results, using a track emulator and supercapacitor. The findings demonstrate that, with appropriate dynamic charge/discharge control, the SOC levels can be adequately managed and no external load or source is required.**

Keywords—electric railways, energy storage system, rail track, regenerative braking, supercapacitor

I. Introduction

Greater reliance on public transportation is an effective means of reducing pollution and global demand for energy derived from fossil fuels. Energy requirements incurred by transportation currently represent about 33% of the total energy consumption in Europe and are responsible for 24% of the total greenhouse gas emissions. Electric railways have been shown to release fewer CO_2 emissions compared to other transportation systems [1], [2]. As a result, the global demand for electric railways has increased, as their benefits include low emissions, reduced noise, and reduced traction energy. However, the increased reliance on electric railways has led to a greater energy consumption, which must be managed to fully capitalise on the aforementioned benefits [3].

Electric railways can be powered by AC or DC voltage. While AC trains are considered faster than DC trains, the latter have the capability to accelerate and decelerate faster than the former. In urban areas, where short distances between interstations are common, rapid acceleration and deceleration is necessary. Therefore, DC traction is preferred [4].

One of the main drawbacks of high acceleration and deceleration that can be achieved by DC are high peaks and dips in the rail network power profiles leading to unstable voltages. Braking trains regenerate power that is used by other trains on the same section of track to meet their power demand, if there is no demand then some of this regenerative power will be dissipated in the form of heat in braking resistors to protect the traction system from overvoltage [5], [6].

Power losses in transmission and braking add to the amount of heat generated inside underground railway tunnels. Higher temperatures on public transport are inconvenient for passengers, especially in the summer. In the London Underground railway system, 85% of the heat inside the tunnels is caused by braking trains that regenerate high power peaks [7], [8]. It has been shown in [9] that installing a line side energy storage system (ESS) will significantly reduce the power losses in the braking resistors, which will in turn help reduce the temperature in underground railways, improving passenger comfort and reducing the cooling cost.

Economic and technical advancements in electric railways can be achieved by efficient use of ESSs. In order to reduce the energy consumption and improve electric railway performance, the energy wasted in the onboard resistors needs to be recovered through the adoption of ESSs. ESS technology has advanced considerably while its cost has also decreased, making it attractive for use in storing the excess energy and injecting it back to the accelerating trains when required. This not only reduces the energy consumption but also helps limit carbon emissions at the source of the electricity supply. Moreover, the stored energy can be used to stabilise the substation voltages by reducing the voltage peaks and dips. In addition, the stored energy can be exploited in emergency to move trains in power outage conditions [10].

Adequate charge/discharge control must be designed for efficient use of a line side ESS. It is important to avoid reaching the maximum and minimum state of charge (SOC) limits, whilst train services are running, as this could diminish the benefits of incorporating ESSs into electric railways. In some applications, the SOC cannot be managed by charging and discharging to an external source (i.e. AC grid) as their only connection is to the track side DC of the power network. There are a number of reasons for this, including: 1) to avoid additional costs of power converters and protection circuits; 2) the most effective locations for an ESS may be between substations and there is no access to an AC grid connection. Discharging to the track when there are no trains on the track to absorb power is restricted due to rectifier only substations with no bi-directional power flow capability. Charging from track when there are no trains running is not possible as the power supplied from the substations are switched off outside of operational hours for track maintenance. Therefore, it is important to design control methods to manage the power flow between the track and the ESS with respect to storage capacity.

In [11] and [12], the SOC of onboard ESSs was controlled using a feed-forward control method to reduce energy consumption. However, the authors assumed that the power profiles of the trains were predictable. It is more challenging when considering the real world case to manage the SOC of lineside ESSs due to a greater uncertainty in the track voltage profiles. As an alternative approach, in [13], the authors presented a numerical optimisation method for controlling the charging and discharging process of a stationary ESS for the purpose of reducing its size. They further considered the impact of their control method on the railway's energy efficiency. Dynamic variation of voltage thresholds based on the train operation states was demonstrated in [14] to be capable of achieving good energy saving.

In this paper, a control algorithm method is proposed to manage the SOC in scenarios characterised by unpredictable train movements and therefore uncertain changes in the track voltage. The aim of the proposed method is to prevent the ESS from reaching the SOC limits whilst maintaining the impact that energy storage can have to reduce energy losses, substation peak power and heat dissipation. This method could also be applied to minimise the ESS capacity required. The work reported in this paper experimentally applies the method to a lab based supercapacitor ESS using a National Instruments (NI) CompactRIO controller and track voltage simulator.

II. The Test Scenario

In this work, ESS technologies are explored by considering a double railway system shown in Fig. 1. In the test scenario, equal distances between adjacent passenger stations are assumed. The diagram depicted in Fig. 1 shows that there are five passenger stations (designated by the letters of the alphabet) separated by 1 km, where the trains stop. The trains' velocities are identical and 180 s headway is assumed between adjacent trains. The traffic scenario is described in Fig. 2. The whole operating time is considered to be one journey which is complete when trains in the upward line finish travelling from A to E and trains in the downward line finish travelling from E to A. The substations' no-load voltage is 600 V and their internal resistance is 20 mΩ. The substations are based on a standard rectifier design and are therefore unidirectional, i.e., that they do not recuperate power when trains brake. The rail electrical resistance is 15 mΩ/km, and the modelling approach described in [15] is adopted.

III. ESS Application

An ideal ESS that is represented by a current source is added next to substation 1 to improve the energy efficiency of the railway model. The output and input energy of the ESS is controlled via a droop controller depicted in Fig. 3. The ESS is charging if the track voltage V_a is higher than or equal to the charging voltage threshold V_{ac}, and it is discharging if it is lower than or equal to the discharging voltage threshold V_{ad}. The ESS is in standby mode if the sensed voltage at its terminals is within the charging and discharging limits. The maximum charging and discharging current limits are denoted by I_{ac} and I_{ad}, respectively. The impact on the terminal voltage at interstation A when charging at 630 V and discharging at 585 V can be seen in Fig. 4. The reduction in voltage peaks results in a reduction in the braking resistors losses, while the reduction in voltage troughs allows lowering the substations' energy consumption and peak power.

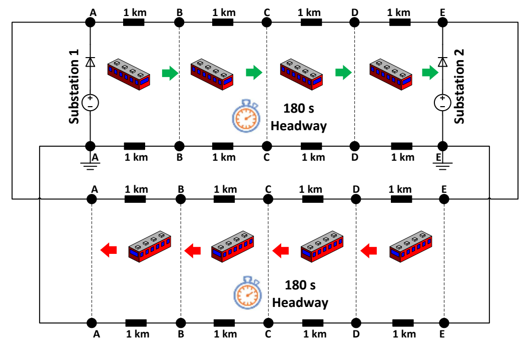

Fig. 1. Double railway track with 2 substations and 8 running trains.

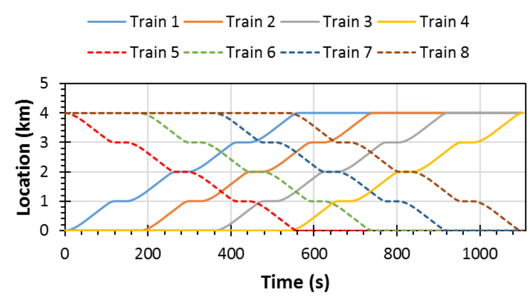

Fig. 2. Train diagrams for a journey including 5 passenger stations.

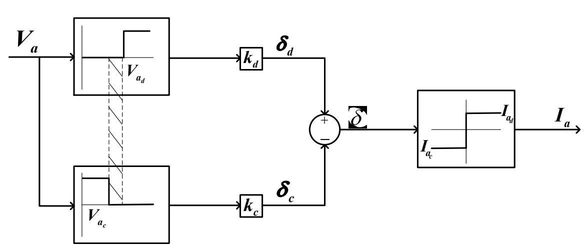

Fig. 3. Voltage control using droop control method.

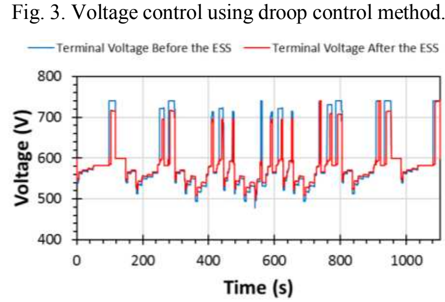

Fig. 4. The terminal voltage at interstation A.

A. SOC Drift

The SOC can be calculated by adopting (1), whereas the SOC drift, defined as the difference between the initial SOC and the final SOC, is calculated by (2).

$$SOC_{out} = SOC(t_\circ) + \frac{\int_{t_\circ}^{t_f} P_{ESS}(t)dt}{3600 \times Q} \quad (1)$$

$$SOC_{drift} = \frac{|SOC(t_\circ) - SOC(t_f)|}{SOC(t_\circ)} \times 100 \quad (2)$$

where Q is the rated ESS capacity, $SOC(t_\circ)$ is the initial SOC, $SOC(t_f)$ denotes the final SOC, and $P_{ESS}(t)$ represents the instantaneous ESS power, which will have positive/negative value during discharging/charging.

B. Voltage Sensitivity

The railway energy efficiency is very sensitive to voltage control, making appropriate voltage threshold selection crucial. Voltage limits should be selected with the objective to reduce the energy consumption of substations and the system power losses. This aim can be met by repeated unbalanced charging and discharging, which causes the SOC at the end of the journey to deviate from the value at the beginning of the journey. As discussed in the introduction it is assumed that the ESS cannot be charged/discharged purely for the purposes of SOC management outside of train operating times. Consequently, there will be a SOC deviation that will result in reaching the maximum and minimum limits of the storage capacity, potentially before the end of an operational period and certainly over a period of repeated days, reducing the effectiveness of the ESS.

A SOC drift sensitivity analysis on varying the charging and discharging voltage threshold for one operating period is shown in Fig. 5. The graph demonstrates the nonlinear relationship between the SOC drift and the voltage limits, with the valley representing the minimum drift. It is important to remain in the vicinity of the valley, which can be achieved by choosing suitable voltage thresholds that also satisfy other energy requirements. However, in practice, the terminal voltage profile in Fig. 4 is not deterministic and exhibits stochastic behaviour according to traffic situations. Therefore, it is essential to design an adaptive controller that can mitigate these uncertainties in the system whilst considering that minimising the SOC drift may have a negative impact on the benefits of the ESS.

C. Control Algorithm

To reduce the SOC drift without adversely affecting the energy efficiency of the electric railway, the control algorithm detailed in Fig. 6 is proposed in this study to allow the voltage and current limits of the droop controller to be modified dynamically. As a result of this approach, if the drift is negative, the charge area in Fig. 7 will expand by adjusting the charging voltage and current limits. The charging voltage will shift closer to the no-load voltage and the charging current will be maximised. Simultaneously, the discharge area will shrink by moving the discharging voltage limit away from the no-load voltage while minimising the discharging current limit. Similarly, the charge area will be compressed and the discharge area will be enlarged if there is a positive drift. The described control method depends mainly on the SOC deviation and the train operating time. Using remaining running time as an input, the higher the deviation and the closer the time to the end of the time, the more responsive the controller becomes.

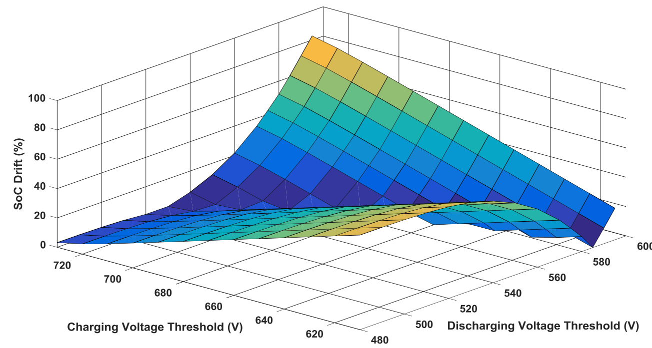

Fig. 5. Absolute value of the SOC drift with respect to variation in voltage limits.

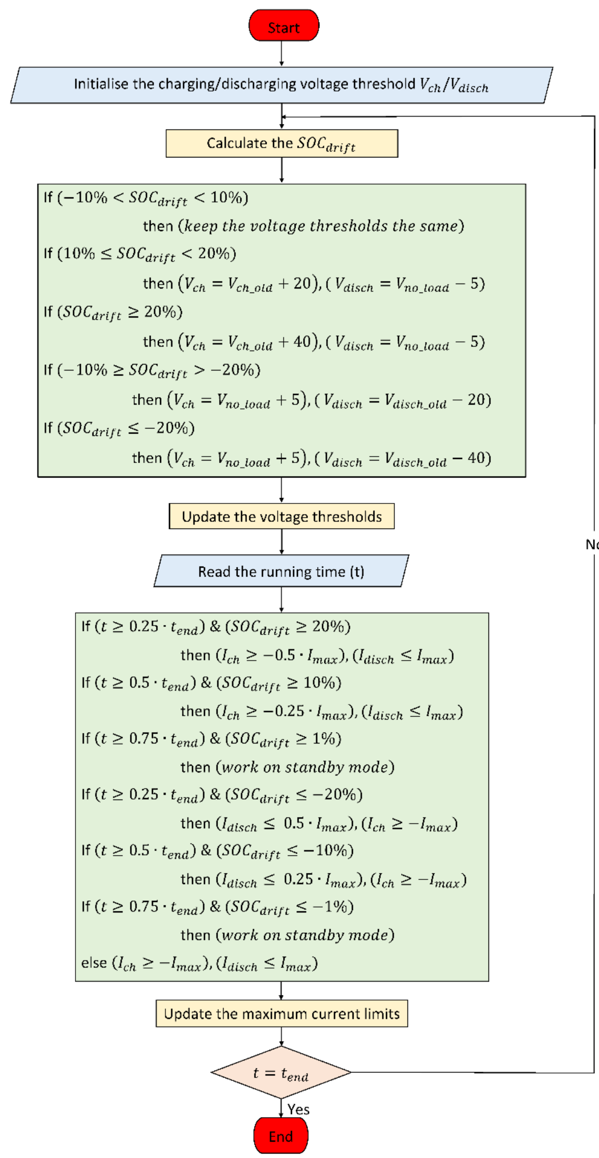

Fig. 6. Flow chart of the SOC drift control.

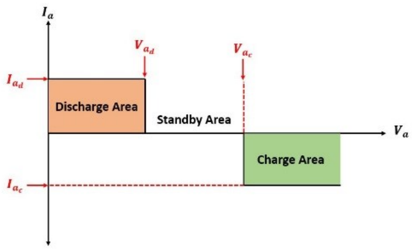

Fig. 7. Voltage and current limit regulation.

IV. Simulation Results

In this section, the impact of the proposed control algorithm on the SOC profile is evaluated against four different scenarios that aim to demonstrate the effects of variations in train journeys. The ESS SOC is limited to a maximum/minimum value of 95% and 5%. The charging/discharging voltage threshold before applying the control algorithm is 630 V/ 585 V. These voltage limits are considered to be effective since they significantly reduce the substations energy demand, substations power peaks, losses in the transmission line, losses in the braking resistors, and SOC drift.

A. Normal Traffic Scenario

When the control algorithm was applied to the described railway model based on the traffic scenario shown in Fig. 2, it successfully minimised the SOC deviation as can be seen in Fig. 8. The total energy saving in the system—which includes the reduction in the substations energy demand, the substations' internal losses, the transmission losses, and the braking losses—was initially 74 kWh, but reduced to 55 kWh after applying the control algorithm. However, these calculations represent the savings for one journey, which cannot be extrapolated to multiple journeys when the SOC is not controlled, because the ESS will reach the capacity limits. This adverse impact will be eliminated by applying the control algorithm, which will certainly increase the energy savings in the long term.

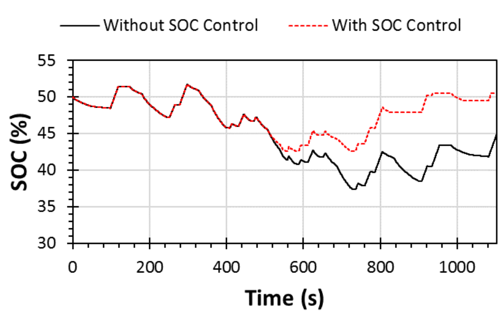

Fig. 8. SOC of the ESS when normal traffic scenario is simulated.

B. Changing Train 2 Headway

In practice, even a small deviation in the headway could result in significant variation in the track voltage and the ESS SOC profiles. Therefore, the ability of the proposed control algorithm to cope with a change in the train 2 headway was examined. For this test, this particular train was set to start 80 s earlier than the scheduled time, which increased the SOC drift significantly before it was controlled (compared to Fig. 8), as can be seen in Fig. 9. The total initial energy saving in the system of 63 kWh declined to 40 kWh after applying the control algorithm.

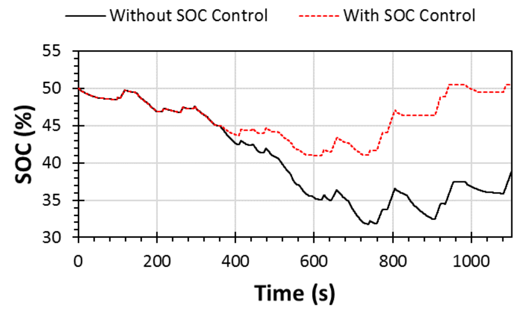

Fig. 9. SOC of the ESS when changing train 2 headway.

C. Stochastic Traffic Scenario

The results reported in the preceding sections were based on ideal traffic conditions, including fixed dwell time, headways, and speed profiles. In this scenario more complex traffic conditions are simulated to test the reliability of the proposed controller. Passengers and drivers introduce random variation to the dwell time, headway, and speed profiles. Therefore, for this test, stochastic headways and speed profiles were adopted. The headway ranged from 2.4 to 6.9 min, while ensuring that a minimum safe distance of 400 m is maintained between consecutive trains when modifying their respective speed profiles. It was further assumed that the number of passengers at stations will increase with the headway. Therefore, the dwell time increased linearly as a function of headway, ranging from 18 s to 58 s. The new traffic scenario is illustrated in Fig. 10. The simulation results demonstrate that the control algorithm was able to cope with the more complex situation, as shown in Fig. 11. However, the total energy saving after the first journey was reduced from 48 kWh to 30 kWh after applying the control algorithm.

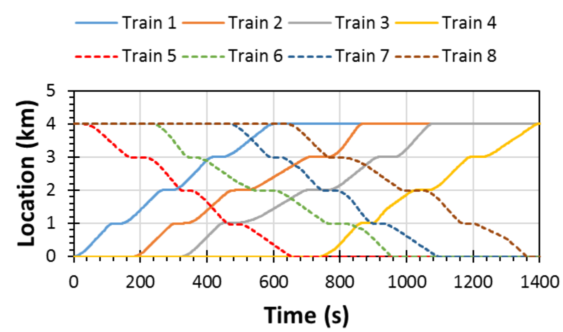

Fig. 10. Train diagrams for the railway system with stochastic behaviour.

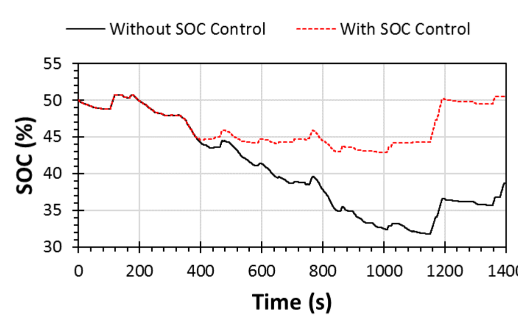

Fig. 11. SOC of the ESS when realistic traffic scenario is applied.

D. Two-Day Simulation

To test the impact of the discussed control method on the railway energy efficiency after multiple journeys, the modelled case described in Section IV.B was simulated for 12 hours per day for two days with a worse case starting condition, $SOC(t_{\circ})$ set to 10%. It can be seen in Fig. 12 that, without SOC control, the ESS repeatedly reaches the lower SOC limit, while the control algorithm is able to avoid this undesirable effect. The figure shows that the SOC fluctuation is highly reduced near the end of first day and near the end of the second day. This is because the control algorithm is designed to be more responsive near the end of each day to make the SOC value close to the desired value 50%. The total energy saving of 3,641 kWh for the two-day operation period without SOC management increased to 3,891 kWh after adopting the management process.

The total energy losses in the railway system represent the sum of the losses in substations, transmission, and braking. Thus far, in all tests, it was assumed that the ESS is ideal and has no internal losses. The braking losses can be considered as a particularly important factor to be minimised by installing the ESS, since their reduction reduces the heat dissipated inside the tunnels, which reduces the need for cooling, and thus the amount of energy imported from the grid. The total energy losses in the system after applying the ESS reduced from 14,411 kWh to 12,299 kWh, and further to 12,113 kWh after applying the SOC control. Most importantly, the ESS reduced the losses in the braking resistors from 6,825 kWh to 4,890 kWh. Thereafter, the control algorithm reduced the braking losses to 4,747 kWh. After multiple days in operation, this reduction will increase even further compared to that potentially achieved without SOC management that cannot avoid operating at low SOC and reaching lower limits. The impact of the discussed control method on the total losses in the system is represented in Fig. 13, depicting a global comparison across different cases.

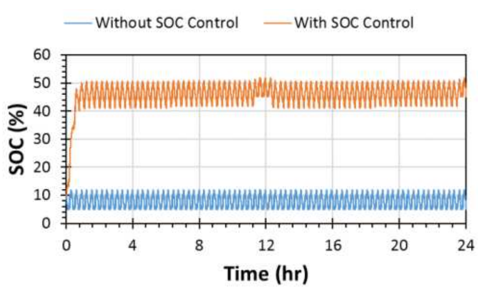

Fig. 12. Two-day simulation based on changing the train 2 headway.

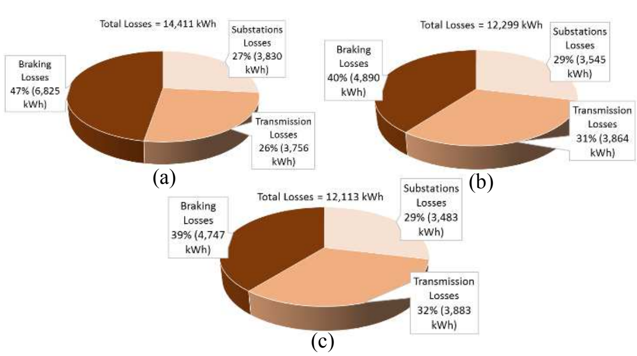

Fig. 13. Total energy losses in the railway system: (a) without ESS; (b) with ESS and no SOC control; and (c) with ESS and SOC control.

V. Experimental Validation

The proposed control method was validated by comparing the simulation results with those obtained experimentally using the test rig shown in Fig. 14. The power converter used in the study is a 30kW Siemens Sinamics DCP DC/DC operating at 600 V. A programmable power supply was connected to one side of the converter to emulate the track voltage. The power was supplied by Zenone Elettronica device that has a maximum voltage of 600 V and a maximum current of 100 A. The terminal voltage profile under the three test conditions was injected into the power supply after scaling the simulated no-load voltage to 400 V to match the Zenone Elettronica capability. The Maxwell supercapacitor was connected to the other side of the converter to represent the ESS. The supercapacitor has a rated capacitance of 63 F, 125 V rated voltage, and 1,900 A maximum current. In the experiment, the supercapacitor voltage was limited to a maximum value of 100 V and it was assumed that the voltage has the same value as the SOC. A NI CompactRIO 9063 was used for data acquisition, transmission, and control and was programmed using LabVIEW. The track voltage and the supercapacitor voltage measurements were measured using the analogue input ports of a NI 9206 module at 100 ms intervals. The DC/DC converter was configured to accept a 0-10V analogue reference for both the voltage and current setpoints. For each update of the control algorithm, the calculated voltage and current setpoints were scaled appropriately to provide the reference signal through the output ports of a NI 9263 module. The maximum sampling rate of the NI 9206 card is 250 kS/s while it is 100 kS/s for NI 9263 card, which provides the high speed and accuracy required for the best performance of the control method. The graphs shown in Fig. 15, Fig. 16, and Fig. 17 show the results of the proposed control method, there is a good fit between the experimental and the simulation results validating the earlier modelling work.

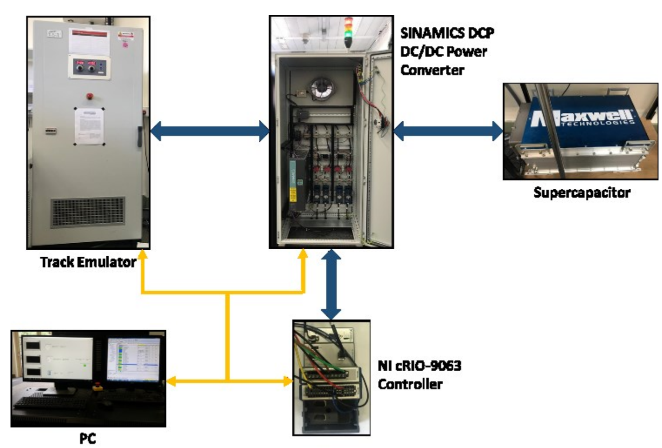

Fig. 14. Hardware setup.

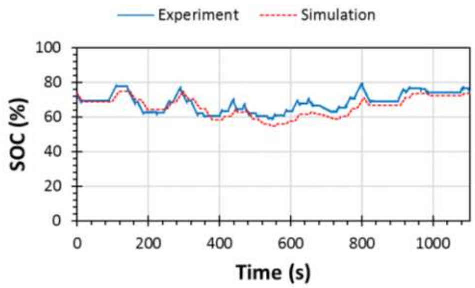

Fig. 15. Experimental ESS results scenario A.

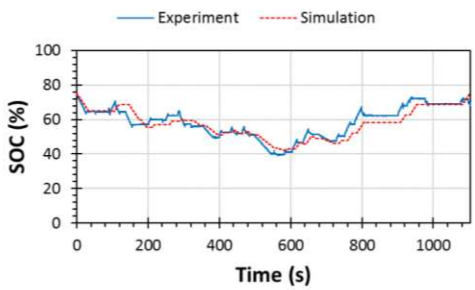

Fig. 16. Experimental ESS results scenario B.

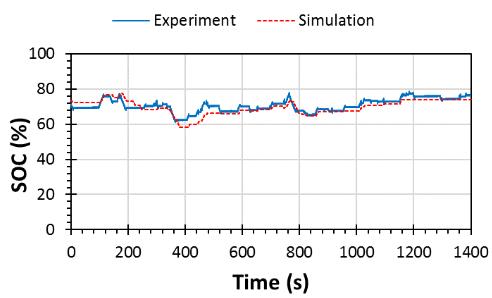

Fig. 17. Experimental ESS results scenario C.

VI. Conclusion

For many ESSs applications in electric railways, the ability to charge/discharge for the purpose of managing SOC will be restricted, this will limit usable capacity of the battery over consecutive operating times. This capacity limitation can reduce the benefits of incorporating ESSs into electric railways. Therefore, an adaptive control technique was developed as a part of this work, aiming to protect an ESS interfaced with a DC electric railway from running out of capacity. Simulation and experimental results pertaining to a number of operating conditions were presented and compared to test the validity of the proposed control methodology. Multiple traffic scenarios including changing the headway, dwell time, and trains speed profiles were applied to add some uncertainty to the system. The proposed controller was demonstrated to be effective under different traffic situations by controlling the SOC via dynamic variation of voltage and current limits. However, the controller lacks predictivity for future changes, which reduces the effectiveness of the ESS in improving the system performance.

A further contribution of this work stems from an experimental implementation of a supercapacitor interfaced with track via a bidirectional DC/DC converter. The control method was implemented in LabVIEW using NI hardware to acquire real time measurements of the supercapacitor voltage, track emulator voltage, and control the DC/DC converter. The obtained findings confirmed that real time voltage and current threshold control can be achieved. A reduction in the system energy efficiency was observed when the controller was implemented over a short duration, however, over longer durations this is not the case as the risk of the ESS being unavailable due to being fully charged or discharged will be mitigated.

References

[1] Eurostat Statistics Explained, “Europe 2020 indicators – climate change and energy,” European Commission, Brussels, Belgium, June 2018.

[2] Eurostat Statistics Explained, “Greenhouse gas emission statistics – emission inventories,” European Commission, Brussels, Belgium, June 2018.

[3] D. Gonzalez, and F. Manzanedo, “Optimal design of a D.C. railway power supply system,” in *2008 IEEE Canada Electric Power Conference*, Vancouver, Canada.

[4] M. Chymera, and C. J. Goodman, “Overview of electric railway systems and the calculation of train performance,” in *IET Professional Development Course on Electric Traction Systems*, London, UK, 2012, pp. 1-18.

[5] A. González-Gil, R. Palacin, and P. Batty, “Sustainable urban rail systems: Strategies and technologies for optimal management of regenerative braking energy,” *Energy Conversion and Management*, vol. 75, pp. 374–388, 2013.

[6] B. Wang, Z. Yang, F. Lin, and W. Zhao, “An improved genetic algorithm for optimal stationary energy storage system locating and sizing,” *Energies*, vol. 7, no. 10, pp. 6434–6458, 2014.

[7] F. Ampofo, G. Maidment, and J. Missenden, “Underground railway environment in the UK part 2: investigation of heat load,” *Applied Thermal Engineering*, vol. 24, no. 5-6, pp. 633-645, Apr. 2004.

[8] A. Revesz, “Modelling of the thermal interactions of underground railways with nearby vertical ground heat exchangers in an urban environment,” PhD Thesis, London South Bank University, 2017. [Online].

[9] H. Alnuman, and D. Gladwin, “Energy storage application into a double DC electric railway,” *Energy Procedia*, vol. 151, pp. 12-16, Oct. 2018.

[10] T. Suzuki, H. Hayashiya, T. Yamanoi, and K. Kawahara, “Application examples of energy saving measures in Japanese DC feeding system,” in *2014 International Power Electronics Conference (IPEC-Hiroshima 2014 – ECCE ASIA)*, Hiroshima, Japan.

[11] R. Takagi, and T. Amano, “Evaluating on-board energy storage systems using multi-train simulator RTSS,” in *IET Conference on Railway Traction Systems (RTS 2010)*, Birmingham, UK.

[12] R. Takagi, and T. Amano, “Optimisation of reference state-of-charge curves for the feed-forward charge/discharge control of energy storage systems on-board DC electric railway vehicles,” *IET Electrical Systems in Transportation*, vol. 5, no. 1, pp. 33-42, 2015.

[13] K. Shiokawa, and R. Takagi, "Numerical optimisation of the charge/discharge characteristics of wayside energy storage systems by the embedded simulation technique using the railway power network simulator RTSS," in *13th International Conference on Design and Operation of Railway Engineering (COMPRAIL 2012)*, Lyndhurst, UK, vol. 127, pp. 583-592.

[14] Z. Yang, Z. Yang, H. Xia, and F. Lin, “Brake voltage following control of supercapacitor-based energy storage systems in metro considering train operation state,” *IEEE Transactions on Industrial Electronics*, vol. 65, no. 8, pp. 6751-6761, 2018.

[15] H. Alnuman, D. Gladwin, and M. Foster, “Electrical modelling of a DC railway system with multiple trains,” *Energies*, vol. 11, no. 11, p. 3211, 2018.